Quantitative evaluation of electro-luminescence images of solar cells

O. Breitenstein[*, 1], **A. Khanna**[2], **Y. Augarten**[3], **J. Bauer**[1], **J.-M. Wagner**[1], and **K. Iwig**[4]

[1] Max-Planck-Institut für Mikrostrukturphysik, Weinberg 2, 06120 Halle, Germany
[2] Institute of Technology, Banaras Hindu University, Uttar Pradesh 221005, India
[3] Centre of Excellence for Advanced Silicon Photovoltaics and Photonics, UNSW, Sydney, New South Wales 2052, Australia
[4] MSC Technik GmbH, Heinrich-Damerow-Straße 2, 06120 Halle, Germany

[*] Corresponding author: e-mail breiten@mpi-halle.mpg.de, Phone: +49-345-5582 740, Fax: +49-345-5511223

A fast converging iterative procedure is proposed to calculate series resistance (R_s) and saturation current (j_0) images from two electroluminescence (EL) images taken at two biases. It is not necessary here that for one bias the influence of the series resistance is negligible. Moreover, voltage series of EL images have been evaluated for calculating images of R_s, j_0, and the parallel conductance G_p separately. However, it has been found that R_s variations cannot uniquely be separated from G_p variations. The reason for this is discussed. Thus, for quantitatively detecting weak ohmic shunts, EL imaging cannot replace lock-in thermography. For strong ohmic shunts a formula for converting EL images into shunt images is given.

Electroluminescence (EL) imaging has been proposed as a method for displaying local variations of the effective diffusion length in solar cells [1]. It has also been used to quantitatively image local variations of the series resistance R_s [2, 3]. These works did not investigate shunted cells. Similar investigations have also been done with photoluminescence imaging [4, 5], but this technique is not so easily applicable as EL since it needs an intense monochromatic illumination source and spectral filtering for the camera. In this contribution, three new approaches for the quantitative evaluation of bias-dependent EL images will be presented. All previous EL evaluation schemes required an R_s-independent image of the local photon yield. Such an image can only be obtained at a low cell bias. Since this image has a low photon yield, a long integration time is needed, and the noise content of this image dominates the signal-to-noise ratio of the results. This limitation can be overcome by the first method presented here. The second method will examine whether an ohmic parallel resistance R_p (or its inverse, the parallel conductance G_p) can be extracted uniquely from bias-dependent EL images.

As with previous EL evaluation schemes [2, 3], this contribution uses the model of a local area-related series resistance $R_{s,i}$ [Ω cm^2] connected in series with a local di-

ode. $R_{s,i}$ is defined by $R_{s,i} = (U - U_i)/j_i$, with U being the applied bias, U_i the local diode voltage and j_i the local dark current density. The local diodes are assumed to have an ideality factor of 1, and diode i is characterized by a local saturation current density of $j_{0,i}$ [A/cm^2]. The ideality factor 1 holds good for biases above 0.5 V, where the diffusion current clearly exceeds the local recombination current. Anyhow, such voltages have to be used for EL imaging for sensitivity reasons. The local EL intensity can be described as $\Phi_i = C_i \exp(U_i/U_t)$ with C_i being a local proportionality factor and U_t the thermal voltage kT/e [2, 3]. Applying the Fuyuki approximation, the proportionality factor C_i of band-to-band transitions scales with the effective diffusion length and thus with $j_{0,i}^{-1}$, for a constant local voltage U_i. This leads to $C_i = f/j_{0,i}$ [1, 3], where f [A/cm^2] is a scaling factor which can be assumed to be the same for all positions, but strongly depends on the experimental conditions (surface roughness, quantum efficiency, integration time of the camera etc.). This leads to the following expression for $U \gg U_t$ as a function of the local EL signal Φ_i [2]:

$$U = U_i + j_i R_{s,i} = U_t \ln(\Phi_i j_{0,i}/f) + \Phi_i R_{s,i} j_{0,i}^2/f . \quad (1)$$

In this equation, U, Φ_i, $j_{0,i}$, and $R_{s,i}$ are implicitly related. $R_{s,i}$ can only be found explicitly if $j_{0,i}/f$ is known. The final

value for $j_{0,i}/f$ is usually obtained from a low voltage calibration EL image where the second term in (1) containing $R_{s,i}$ is expected to be negligible [3]. The question is, which error is caused by neglecting the second term of (1) in the calibration image? In practice a compromise must be chosen between obtaining a good signal-to-noise ratio and minimizing the influence of $R_{s,i}$. In the "ISE method" of Haunschild et al. [3] the factor f was chosen so that the arithmetic mean value of $R_{s,i}$ equals the global R_s value of the cell. However, they still observed some minor influence of $j_{0,i}$ in $R_{s,i}$ which was probably due to the non-ideal conditions of the calibration measurement. $j_{0,i}$ was not evaluated quantitatively in [3].

The first approach presented in this letter is based on two EL measurements taken at two different voltages U_1 and U_2, which both have sufficiently high EL signals. Note that here a Si CCD camera was used which detects only band-to-band luminescence. The influence of $R_{s,i}$ on U_i is calculated for both measurements by applying the following iteration scheme: In the first approximation, the local voltages of the first measurement $U_{i,1}$ are assumed to be the applied voltage for this measurement (i.e. the ISE approximation [3]; $U_{i,1}^{(1)} = U_1$). Neglecting the R_s term in (1) leads to

$$j_{0,i}^{(1)} = \frac{f}{\Phi_{i,1}} \exp \frac{U_{i,1}^{(1)}}{U_t}. \qquad (2)$$

The first approximation for $R_{s,i}$ is calculated from the second EL image (taken at a voltage U_2), using (1):

$$R_{s,i}^{(1)} = \frac{f}{\Phi_{i,2}(j_{0,i}^{(1)})^2} \left(U_2 - U_t \ln \frac{\Phi_{i,2} j_{0,i}^{(1)}}{f} \right). \qquad (3)$$

The second approximations for the local voltages of the first image ($U_{i,1}^{(2)}$) are then calculated using these R_s values, by

$$U_{i,1}^{(2)} = U_1 - R_{s,i}^{(1)} j_{0,i}^{(1)} \exp \frac{U_{i,1}^{(1)}}{U_t}. \qquad (4)$$

This loop (2)–(4) is then repeated several times. We have found that convergence to an accuracy below 0.1% occurs within 10–20 iterations, taking only seconds. As with the ISE method, the scaling factor f may be chosen so that the mean value of $R_{s,i}$ equals the global R_s value of the cell. Alternatively, also the mean value of $j_{0,i}$ may be fitted to the global value of the diffusion current density J_{01}.

This iterative procedure has been tested on a typical 156×156 mm^2 sized industrial multicrystalline cell. The result was compared to the result of the ISE method, which is the first iteration step of our method. Analysis of the dark $J–U$ characteristic of this cell gave a global value of $R_s = 0.49$ Ω cm^2 and a global diffusion current density of $J_{01} = 1.2 \times 10^{-12}$ A/cm^2. Two first EL images were taken at voltages of $U_{1a} = 0.55$ V and $U_{1b} = 0.59$ V, with currents of 0.55 A and 1.93 A, respectively. The second EL image was taken at $U_2 = 0.63$ V, with a current of 6.43 A. All integration times were 1 min. For both the ISE method and our iterative method the results using $U_1 = 0.55$ V and

$U_2 = 0.63$ V agreed well with each other, but showed an inferior signal-to-noise ratio. For $U_1 = 0.59$ V and $U_2 = 0.63$ V our method led to the same results, in contrast to the ISE method. Figure 1 compares the results for $U_1 = 0.59$ V and a value of $f = 1.5 \times 10^{-19}$ A/cm^2 for both methods.

Figure 1 shows that for the ISE method the averaged R_s values (a) are 44% lower than obtained by us (b), and the j_0 values (c) are 9% increased compared to (d). Moreover, the j_0 image of this 1st iteration is clearly influenced by the R_s image, which is not the case for the 20th iteration (d). For the chosen value of f, not only does the average value of R_s in (b) equal the globally measured one, but the average value of j_0 of 1×10^{-12} A/cm^2 is also close to the 1.2×10^{-12} A/cm^2 estimated from the global $J–U$ characteristic. Thus, our method may be considered as an alternative to the j_0 imaging technique proposed recently by Glatthaar [6]. The local maxima in the j_0 images are recombination-active grain boundaries and linear and non-linear local shunts. It has been found by lock-in thermography investigations that only the uppermost and the lowermost bright spots in the j_0 images are ohmic shunts (see arrows in (d)), the other shunts are non-linear. In the positions of the shunts the displayed j_0 shows local maxima and R_s shows local minima. The R_s minima are artefacts coming from the assumption of an ideality factor of 1, which does not hold in shunt positions, but the j_0 maxima may be real for the non-linear shunts.

The question still remains whether EL is also able to image ohmic shunts reliably. From simulations and experiments it has been found that only stronger ohmic
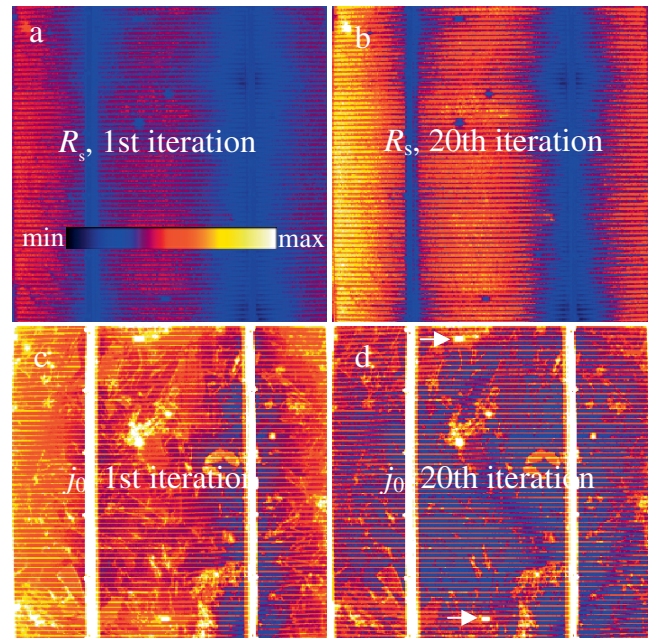

Figure 1 (online colour at: www.pss-rapid.com) R_s images (a, b, max value is 1.5 Ω cm^2) and j_0 images (c, d, max value is 1.2×10^{-12} A/cm^2) based on EL images at 0.59 V and 0.63 V. Left (a, c) first iteration (ISE method); right (b, d) after 20 iterations.
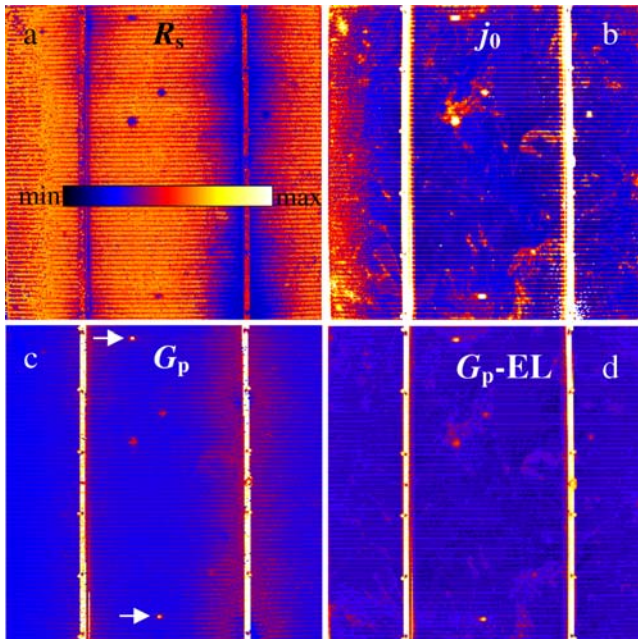
Phys. Status Solidi RRL **4**, No. 1 (2010)

9

Figure 2 (online colour at: www.pss-rapid.com) a) R_s image, max value is 1.5 Ω cm^2, b) j_0 image, max value is 1.2×10^{-12} A/cm^2, c) G_p image, max 0.1 S/cm^2, d) "G_p-EL" image, max 0.2 S/cm^2.

shunts can uniquely be distinguished from other recombination-active defects [7, 8]. If a resistance $R_{\text{p},i}$ (Ω cm^2) is connected in parallel to the local diode i, (1) extends to [2]

$$U = U_\text{t}(1 + R_{\text{s},i}/R_{\text{p},i}) \ln\left(\Phi_i j_{0,i}/f\right) + \Phi_i\, R_{\text{s},i}\, j_{0,i}^2/f \ . \qquad (5)$$

We have numerically fitted 11 EL images measured between $U_\text{min} = 0.54$ V and $U_\text{max} = 0.638$ V to (5) by using a specially developed iteration method, different from that previously described, to calculate separate images of R_s, j_0, and the ohmic conductance $G_\text{p} = 1/R_\text{p}$. For our images of 256×256 pixels this procedure took about 1 h on a standard PC. The results are shown in Fig. 2a–c, where the R_s image (a) and the j_0 image (b) are displayed in the same scaling as in Fig. 1. It was hoped that the G_p image (c) would predominantly show the two ohmic shunts in this cell.

It turned out that even under the best fitting conditions the G_p image not only reveals the local ohmic shunts (see arrows) but also the non-linear shunts. It also shows a clear anti-correlation to the R_s image, which is obviously an artifact. Again, R_s shows artificial local minima at shunt positions. We believe that the inability of this procedure to reveal only the ohmic conductivity in the G_p image, independent of R_s, is a fundamental mathematical problem: Both R_s and G_p tend to linearize the originally exponential Φ–U characteristic in a similar manner. Therefore the fitting procedure cannot uniquely distinguish between local variations of R_s and G_p. The procedure is also influenced by the inevitable experimental noise, accidentally attributing certain variations of the Φ–U characteristic to either R_s or to G_p variations. Indeed, manual fitting of experimental

data points has shown that the same data set can be fitted with the same accuracy both with and without an ohmic conductance. Fitting with the ohmic conductance results in lower R_s and higher j_0 values. Thus, this procedure cannot be proposed for general quantitative use. This was an interesting result, which should be presented here.

In order to at least approximately evaluate stronger ohmic shunts in EL images quantitatively, we propose a third method which assumes homogeneous values for $R_{\text{s},i} \equiv R_\text{s}$ and $C_i \equiv C$ and evaluates only one EL image. This EL image should be taken at low voltage to reduce the influence of R_s outside of shunts. Then, in the presence of an ohmic shunt whose conductivity $G_{\text{p},i}$ is larger than that of the local diode, the local voltage is given by $U_i = U/(R_\text{s}G_{\text{p},i} + 1)$. Using $\Phi_i = C \exp(U_i/U_\text{t})$ and the average value $\bar{\Phi} = C \exp(\bar{U}/U_\text{t})$, with $\bar{U} \approx U$ (only local shunts), this can be written as

$$G_{\text{p},i} = \left(1/\left[1 - (U_\text{t}/U)\ln(\bar{\Phi}/\Phi_i)\right] - 1\right)/R_\text{s} \ . \qquad (6)$$

Figure 2(d) shows the resulting "G_p-EL" image calculated from the 0.55 V EL image. Like the G_p image from the iteration (c), this image looks similar to the DLIT image and clearly shows the ohmic shunts. It does not reveal R_s variations but still contains residual j_0 contrast. It shows the ohmic shunts about a factor of 2 stronger than the special iteration method because the latter erroneously attributes G_p variations partly to a reduced R_s and an increased j_0. This method still can be improved e.g. by considering the locally varying R_s [7].

In this Letter new methods for quantitatively evaluating bias-dependent EL images are introduced, which may extend the application field of EL imaging in solar cell characterization. The j_0 image can also be displayed as an effective diffusion length or lifetime image. It has been found that, under the assumption of a local diode ideality factor of 1, a complete EL evaluation cannot uniquely distinguish between ohmic shunts, series resistance changes, and other local recombination-active defects. A new formula for quantitatively displaying stronger ohmic shunts from one EL image has been presented.

References

[1] T. Fuyuki et al., Appl. Phys. Lett. **86**, 262108 (2005).
[2] D. Hinken et al., Appl. Phys. Lett. **91**, 182104 (2007).
[3] J. Haunschild et al., Phys. Status Solidi RRL **3**, 227 (2009).
[4] T. Trupke et al., Appl. Phys. Lett. **93**, 093506 (2008).
[5] H. Kampwerth et al., Appl. Phys. Lett. **93**, 202102 (2008).
[6] M. Glatthaar et al., J. Appl. Phys. **105**, 113110 (2009).
[7] M. Kasemann et al., Prog. Photovolt., Res. Appl. **16**, 279–305 (2008).
[8] O. Breitenstein et al., Prog. Photovolt., Res. Appl. **16**, 325–330 (2008).